

Generation of amorphous silicon structures by rapid quenching: A molecular-dynamics study

Manabu Ishimaru, Shinji Munetoh, and Teruaki Motooka

Department of Materials Science and Engineering, Kyushu University, Hakozaki, Fukuoka 812-81, Japan

(Received 24 June 1997)

Amorphous silicon (*a*-Si) networks have been generated from melted Si with various quenching rates by molecular-dynamics (MD) simulations employing the Tersoff potential. The cooling rates were set between 5×10^{11} and 1×10^{14} K/s; the latter is the slowest quenching rate in MD simulations previously performed. Although the atomic configurations formed by the cooling rate of 10^{14} K/s could reproduce the radial distribution function of *a*-Si obtained experimentally, they contained numerous structural defects such as threefold- and fivefold-coordinated atoms. As the cooling rate decreased, the average coordination number became ≈ 4 and tetrahedral bonds predominated. The structural and dynamical properties of *a*-Si generated by a cooling rate with $\sim 10^{12}$ K/s were in excellent agreement with those of *a*-Si obtained experimentally. [S0163-1829(97)00547-X]

I. INTRODUCTION

The determination of the microstructure of amorphous silicon (*a*-Si) is of great importance for electronic device applications of *a*-Si. A molecular-dynamics (MD) simulation is a useful technique to obtain atomic-scale information on the *a*-Si structure, and many researchers have proposed the preparation methods of *a*-Si based on MD simulations.¹ Recently, Car and Parrinello² and Stich, Car, and Parrinello³ generated *a*-Si from melted Si, employing *ab initio* MD simulations in which the volume of the MD cell was gradually increased by applying negative pressure. The structural, dynamical, and electronic properties of the computer-generated *a*-Si were in good agreement with those obtained experimentally.⁴⁻⁶ However, *ab initio* MD simulations are numerically so intensive that they are limited to a short period of time (~ 10 ps) and small numbers of atoms (~ 100). Therefore, it is difficult to apply *ab initio* MD simulations for the analysis of relaxation and crystallization processes in *a*-Si, where much larger-size simulations in space and time are necessary.

To overcome this problem, various empirical interatomic potentials for Si have been proposed.⁷ Luedtke and Landman^{8,9} tried to produce *a*-Si by rapid quenching of the liquid using an empirical potential developed by Stillinger and Weber.¹⁰ In their MD simulations, the strength of the three-body term in the potential is artificially enhanced during the cooling procedure in order to stabilize the tetrahedral structure. Thus the kinetics of quenching may not be well described. In addition, the Stillinger-Weber (SW) potential, which is often used to analyze the microstructure of liquid Si (*l*-Si) and *a*-Si, has been pointed out not to reproduce exactly the structural and dynamical properties of the liquid phase of Si.¹¹

Although much effort has been devoted to construct structural models of *a*-Si, the preparation methods of *a*-Si involve unphysical treatments and the details of the microstructures are not yet fully examined. We have recently performed MD simulations of *l*-Si using the Tersoff potential^{12,13} instead of the SW potential and found that the *l*-Si network generated reproduces the features of the structural properties reported

by previous experiments and *ab initio* calculations.^{14,15} In the present study, *a*-Si networks were generated from the Tersoff liquid by various cooling rates. The structural and dynamical properties of the calculated atomic configuration were compared with those reported by previous experiments and *ab initio* calculations and the applicability of the Tersoff potential for preparing *a*-Si was discussed.

II. PREPARATION PROCEDURE OF AMORPHOUS SILICON

Cook and Clancy¹⁶ have conducted constant-pressure MD simulations of the solid-liquid transition using the Tersoff potential and found that the density of computer-generated *l*-Si is substantially different from that obtained experimentally. In the present study, therefore, the MD calculations were carried out under constant-volume and -temperature conditions. A cubic cell with periodic boundary conditions contains $N = 216, 512,$ and 1000 Si atoms interacting via the Tersoff potential.¹³ The density of the MD cell was chosen as that of crystalline Si (*c*-Si), namely, 2.33 g/cm^3 , since the density of *a*-Si without voids is close to that of *c*-Si. The atoms were initially arranged in the diamond structure and then the system was heated up by rescaling the velocities of the particles. The equations of motion were integrated using the velocity form of the Verlet algorithm¹⁷ with a time step of 0.002 ps.

The amorphous state was obtained by first equilibrating *l*-Si at a high temperature of 3500 K and then quenching it to 500 K. The cooling rates were set between 5×10^{11} and 1×10^{14} K/s. The slowest cooling rate of 5×10^{11} K/s in the present study was about 200 times slower than that used in the previous *ab initio* MD simulations ($\sim 10^{14}$ K/s) (Ref. 3) and almost the same as the estimated cooling rates that were achieved in laboratories to prepare *a*-Si by laser annealing techniques ($\sim 10^{12}$ K/s).¹⁸

III. RESULTS AND DISCUSSION

Figure 1 shows examples of (a) kinetic and (b) potential energies of an $N = 512$ system as a function of time with the

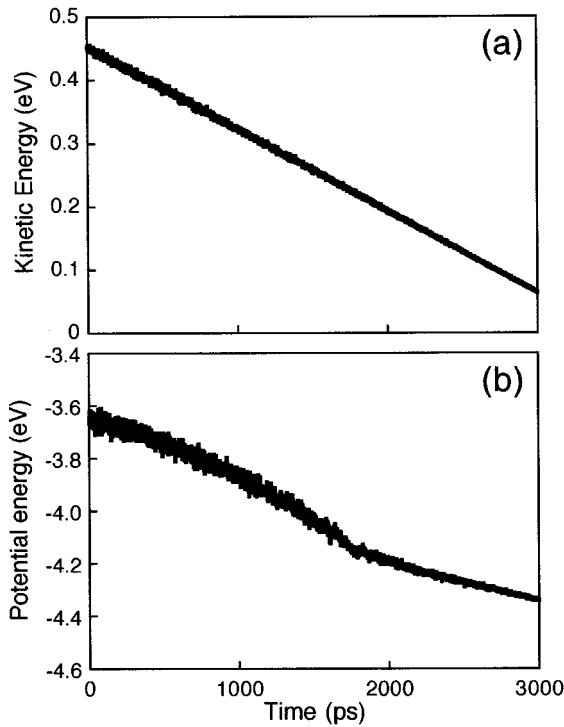


FIG. 1. Time evolution of (a) kinetic and (b) potential energies per particle during quenching. The system is $N=512$ and the cooling rate is 1×10^{12} K/s. It should be noted that the potential energy has a kink around 1800 ps corresponding to a temperature of 1700 K, though the kinetic energy decreases monotonically.

cooling rate of 10^{12} K/s. It should be noted that *l*-Si is simply quenched without any *ad hoc* procedures such as the application of negative pressure and the enhancement of tetrahedral force components during the cooling procedures as described in Sec. I. There exists a kink in the potential energy around 1800 ps during the cooling. For comparison with the other cooling rates examined, the temperature dependence of the potential energy is shown in Fig. 2. [This

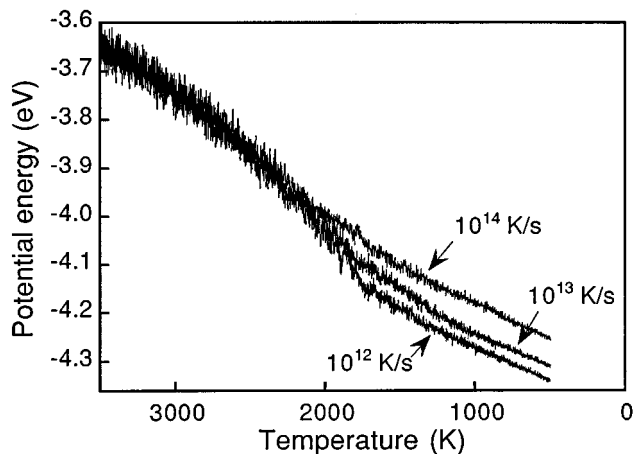


FIG. 2. Temperature dependence of the potential energies for various quenching rates. Note that the kink exists around 1700 K for 10^{12} K/s and its position moves toward higher temperature with increasing cooling rate.

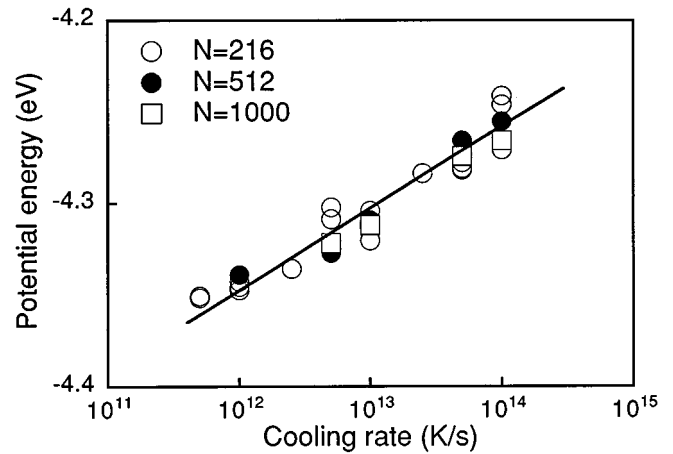


FIG. 3. Equilibrium potential energy at 500 K for various cooling rates: $N=216$ (\circ), $N=512$ (\bullet), and $N=1000$ (\square). The line is a guide to the eye. The potential energy decreases monotonically with quenching rate.

picture is obtained by converting the horizontal axis of Fig. 1(b) into the temperature.] It is found that the kink appears around 1700 K for 10^{12} K/s and it shifts toward higher temperature and disappears as the quenching rate increases. The temperature at which the kink appears was confirmed to slightly decrease in the case of $\leq 10^{12}$ K/s (not shown). This kink may correspond to the enthalpy change 34.3 ± 4.2 kJ/mol upon melting of *a*-Si observed experimentally.¹⁹

Figure 3 displays the potential energy at 500 K for various quenching rates. One can see that the values do not depend on the system size, therefore the present size ($N=512$) is considered to be large enough. The potential energy decreases with the cooling rate. This suggests that numerous defects, such as atoms with under- or overcoordination numbers, exist in *a*-Si generated by the rapid freezing and these defects can recover at slower cooling rates.

From the slope of potential-energy curve for 10^{12} K/s (Fig. 2), the cooling procedure can be divided into three parts: (i) 3500–2300 K, (ii) 2300–1700 K, and (iii) 1700–500 K. In order to obtain information about atomic arrangements for each temperature range, the radial distribution functions $g(r)$ of the samples quenched at 2700, 2000, and 500 K are demonstrated in Fig. 4. In Fig. 4(a) the first peak falls at 2.46 \AA with a maximum height of 2.3 and the second one appears at 3.94 \AA . This $g(r)$ is essentially similar to that calculated previously in the Tersoff liquid.¹⁴ The peaks become sharper as temperature decreases [Fig. 4(b)] and finally the location of the first peak is close to that of *c*-Si (2.35 \AA) and the minimum region between the first two peaks becomes deep [Fig. 4(c)]. It should be noted that the third-nearest-neighbor peak of *c*-Si (4.50 \AA) is not observed. These results of Fig. 4(c) reproduce the features of *a*-Si generated experimentally well.^{4,5} Although $g(r)$ of the sample prepared by 10^{14} K/s is similar to that obtained by 10^{12} K/s, the peak heights are a little smaller as shown in Fig. 4(c).

To compare with the available data of neutron-diffraction measurements,^{4,5} the static structure factors $S(k)$ calculated by Fourier transforming $g(r)$ are given in Fig. 5. The k

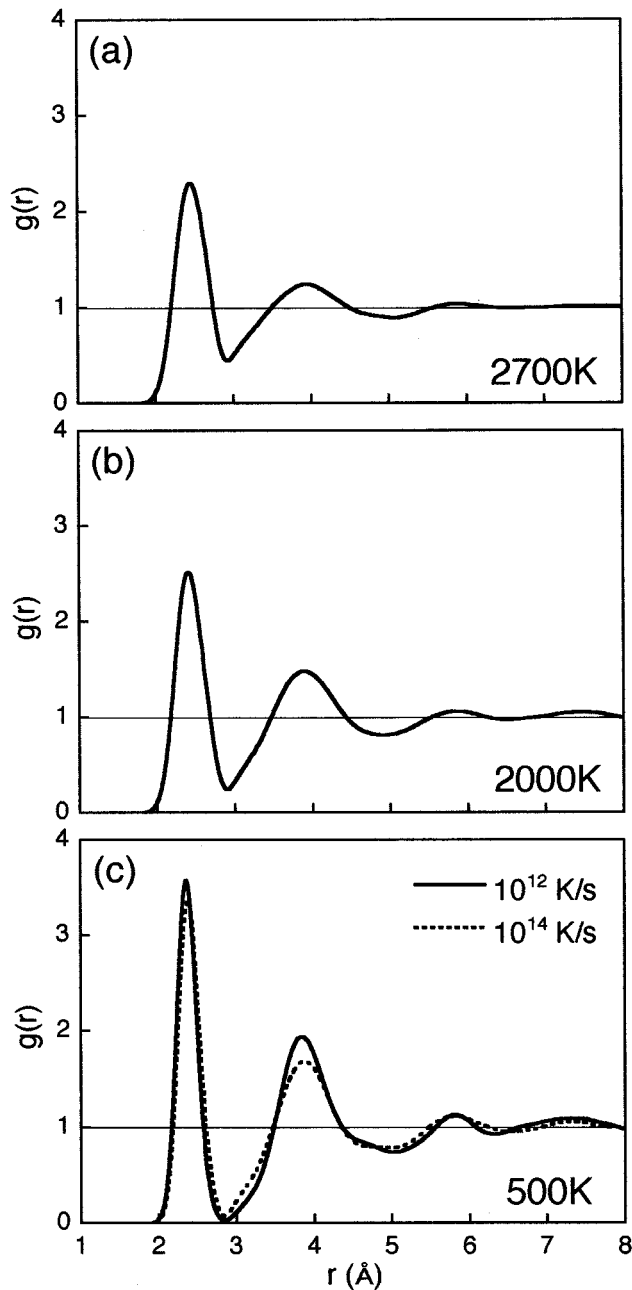


FIG. 4. Temperature dependence of radial distribution functions $g(r)$: (a) 2700, (b) 2000, and (c) 500 K. Solid and dotted lines denote the cooling rates of 10^{12} and 10^{14} K/s, respectively. These functions are obtained by averaging over 500 configurations during $500\Delta t$ (1.0 ps).

$<1.5 \text{ \AA}^{-1}$ region contains substantial truncation error and should be disregarded. It is clearly seen that the first peak is asymmetric in Fig. 5(a) and the peak shape resembles that of $S(k)$ for a supercooled liquid.¹¹ (Note that the melting temperature is about 3300 K for the system with the density of 2.33 g/cm^3 used in the present MD simulation.) This first peak splits into two and these peaks develop with decreasing temperature. The result of 10^{12} K/s in Fig. 5(c) is in excellent agreement with that obtained experimentally from evaporated $a\text{-Si}$.⁴ On the other hand, $S(k)$ for the cooling rate of

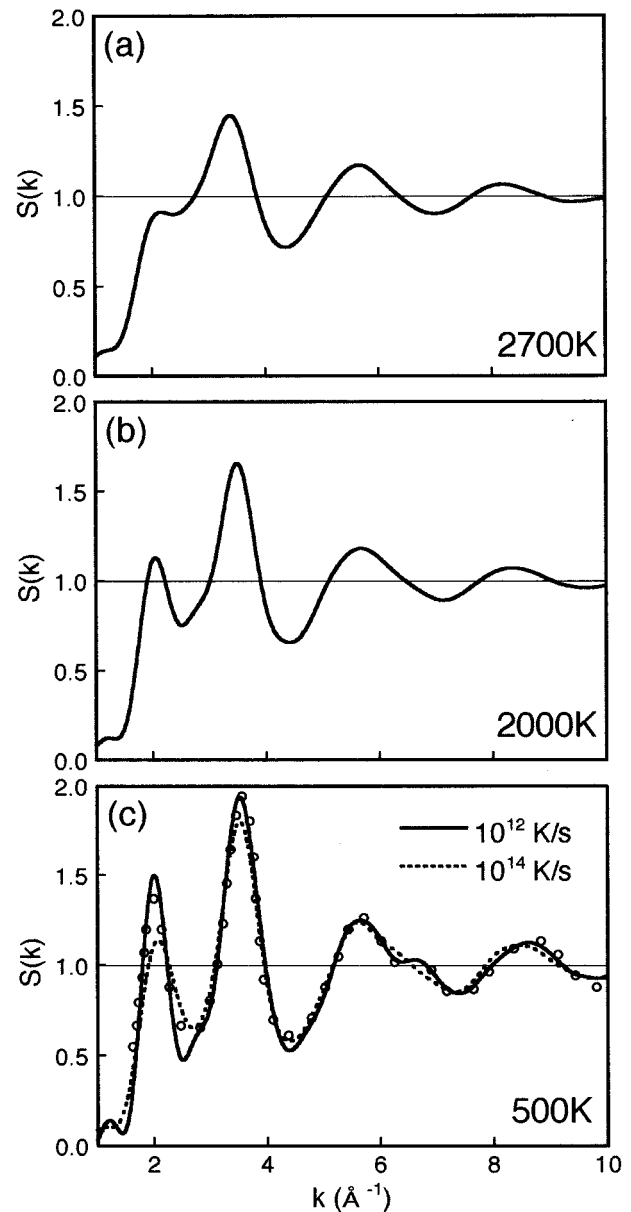


FIG. 5. Static structure factors $S(k)$ corresponding to Fig. 4: (a) 2700, (b) 2000, and (c) 500 K. Solid and dotted lines denote the cooling rates of 10^{12} and 10^{14} K/s, respectively, and open-circle indicates an experimental result reported by Fortner and Lannin (Ref. 4). The $S(k)$ for 10^{12} K/s in (c) reproduces the experimental result well.

10^{14} K/s includes some discrepancies in the height of the first peak and the shoulder of the third peak. Therefore, the quenching rate needs to be below 10^{12} K/s for the formation of a more appropriate amorphous structure.

Figure 6 indicates the distribution of coordination numbers as a function of temperature. The coordination shell is defined by the first minimum of $g(r)$. At 2700 K various coordination numbers composed of primarily fourfold and fivefold coordinations exist. The fourfold coordination predominates at the lower temperatures, and the threefold sites vanish and only fivefold ones remain for the cooling of 10^{12} K/s. The sample produced by 10^{14} K/s also includes

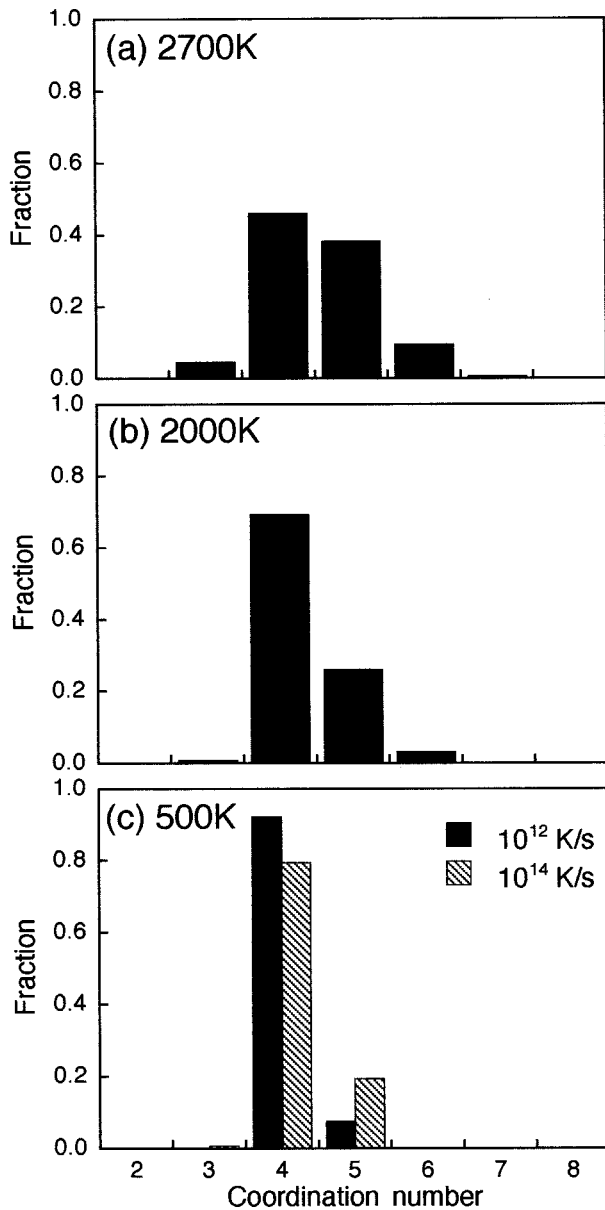


FIG. 6. Distribution of coordination numbers for various temperatures during the cooling: (a) 2700, (b) 2000, and (c) 500 K. It should be noted that primary defects consist of atoms with fivefold coordination.

many floating bonds (19.5%) rather than dangling bonds (0.8%). According to continuous-space Monte Carlo simulations by Kelires and Tersoff,²⁰ the estimated formation energies for fivefold-coordinated defects are smaller than those for the threefold-coordinated defects, which is consistent with the present MD results. A similar tendency in the distribution of coordination numbers as a function of temperature has been found also by Stich, Car, and Parrinello.³ The average coordination decreases monotonically with the cooling rate and the value is close to the coordination number of *c*-Si, 4.0 (Fig. 7).

Typical spin densities of *a*-Si determined by electron-spin-resonance (ESR) measurements are 10^{18} – 10^{20} cm⁻³ and the dominant structural defect in *a*-Si is believed to be

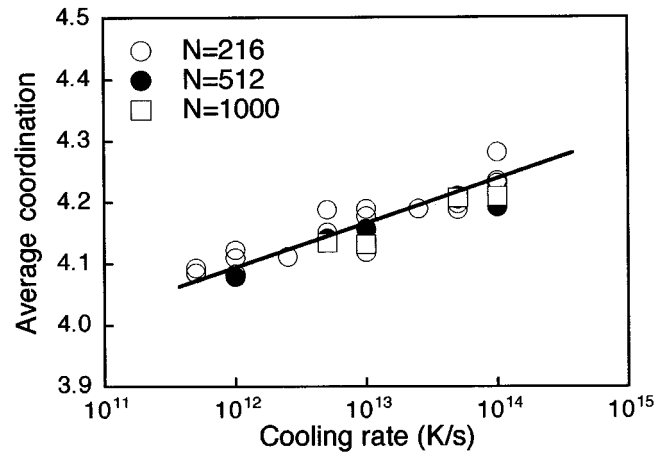


FIG. 7. Change in average coordination number for various quenching rates: $N=216$ (○), $N=512$ (●), and $N=1000$ (□). The line is a guide to the eye. With a decrease of cooling rate, the average coordination number is close to 4.

the threefold-coordinated atom, known as the dangling bond. Our *a*-Si consists of only 1000 atoms; therefore it is reasonable that the threefold sites cannot be observed as shown in Fig. 6(c). Our simulations indicate that the fivefold-coordinated atoms are possible intrinsic defects in *a*-Si, which is consistent with the results obtained by earlier simulations.^{8,9,20,21} If the fivefold sites are not ESR active, there is no discrepancy between the computer-generated and real *a*-Si structures. However, Pantelides²² has suggested that the fivefold-coordinated atoms or floating bonds can be ESR active sites. Therefore, more detailed discussions are needed to clarify the dominant structural defect and ESR active site in *a*-Si. It seems that *ab initio* MD simulations including spin-polarization effects are useful for the analysis of native defects in *a*-Si. Actually, Stich, Parrinello, and Holender²³ have pointed out that the inclusion of spin has appreciable effects on the description of the bond breaking and forming processes, which improves the description of the structural and dynamical behavior of *l*-Si.

Figure 8 illustrates the temperature dependence of the bond angle distribution functions $g(\theta)$. The cutoff distance to characterize a bond is set at the first minimum position in $g(r)$. There exist two peaks around 60° and 100° in Fig. 8(a). The 60° peak becomes small at 2000 K, as shown in Fig. 8(b), because it originates from atoms with the overcoordination.¹⁵ At 500 K, $g(\theta)$ is close to a Gaussian distribution centered around the tetrahedral angle and the 60° peak remains in the case of rapid quenching ($\geq 10^{16}$ K/s). This suggests that *l*-Si transforms into glass for rapid quenching rates. From the analysis of radial distribution functions of as-deposited *a*-Si samples, Fortner and Lannin⁴ have estimated that the peak position and the standard deviation of bond angles are $\bar{\theta}=108.4^\circ$ and $\sigma_\theta=11.0^\circ$, respectively. These values are in good agreement with those obtained by the present simulation ($\bar{\theta}=108.7^\circ$ and $\sigma_\theta=13.5^\circ$).

In order to clarify the dynamical properties of *a*-Si generated by the Tersoff potential, the phonon densities of states (PDOS's) were calculated from the Fourier transform of the velocity autocorrelation functions (see Fig. 9). The PDOS

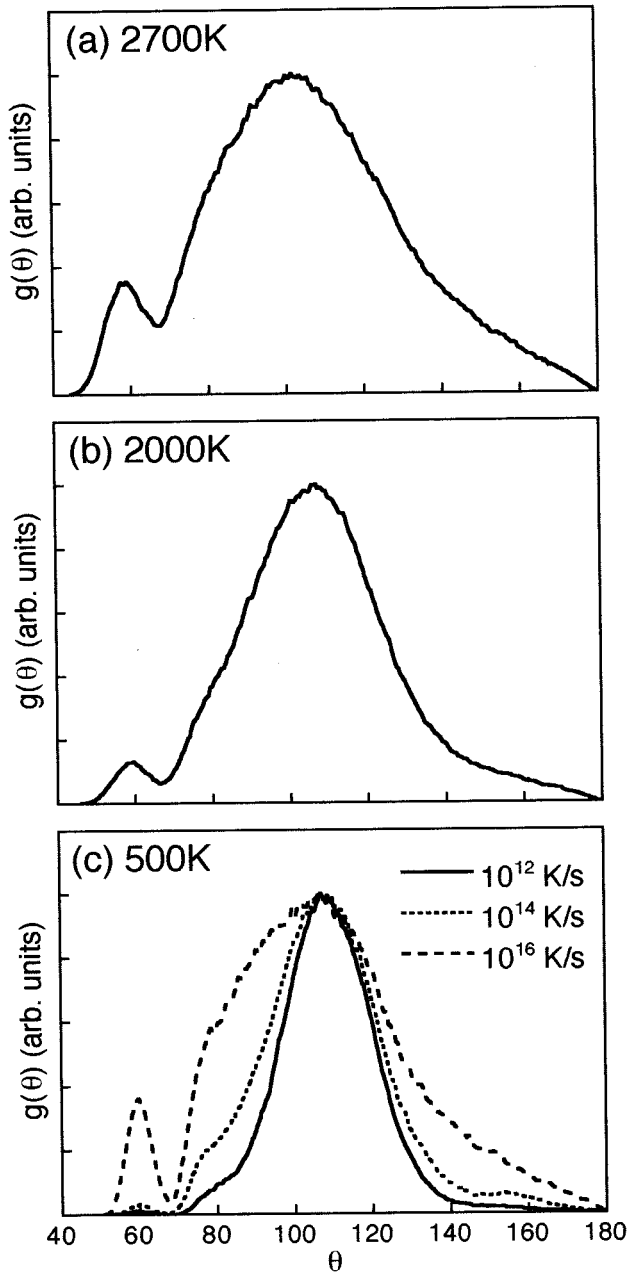


FIG. 8. Bond angle distribution functions $g(\theta)$ for the atomic arrangements at (a) 2700, (b) 2000, and (c) 500 K. The peaks exist around 60° and 100° in (a). With decreasing temperature, the peak center shifts toward the tetrahedral angle and the 60° peak disappears in (c).

becomes zero at $\omega=0$, therefore microdiffusion and atomic rearrangements do not exist in our sample, which can be also seen in as-quenched a -Si of *ab initio* MD simulations.³ The peaks around 20, 40, and 60 meV correspond to the acoustic and optical vibrational modes of c -Si. These positions are in good agreement with the experimental ones indicated by open circles,²⁴ suggesting that a -Si generated from the Tersoff liquid can reproduce not only the static structures but also dynamical properties of actual a -Si.

From our previous^{14,15} and present MD simulations, it is suggested that the Tersoff potential can be systematically

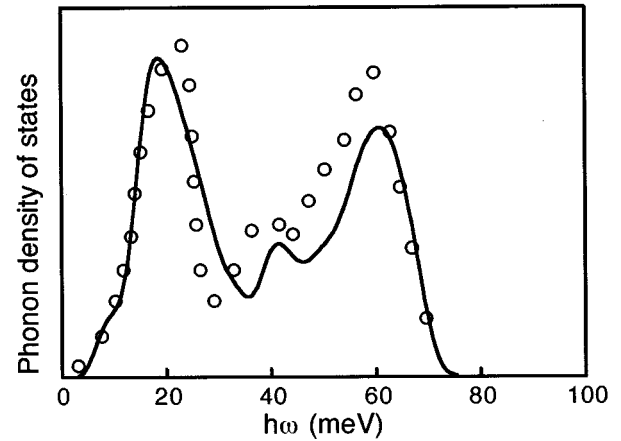


FIG. 9. Phonon density of states of a -Si obtained by the cooling rate of 10^{12} K/s. Open circles indicate an experimental result reported by Kamitakahara *et al.* (Ref. 24).

employed for the analysis of the structural and dynamical properties of c -, a -, and l -Si. Therefore, based on this empirical potential, it is possible to conduct further investigations, such as the relaxation and crystallization processes of a -Si and the mechanism of the solid-phase epitaxial growth. More extensive study is currently under way.

IV. CONCLUSION

The structural and dynamical properties of a -Si have been investigated by using MD simulations; the following conclusions have been reached.

(i) We succeeded in the formation of the a -Si structure without the artificial procedure that is involved in previous MD simulations. It was confirmed that the structures of l -Si are frozen in the cooling rate of $\geq 10^{16}$ K/s, while a tetrahedral network is recovered at $\leq 10^{12}$ K/s.

(ii) The static and dynamical behaviors of a -Si generated by the Tersoff empirical potential were in excellent agreement with those obtained by experiments. This represents that the Tersoff potential is sufficient for the structural analysis of a -Si.

(iii) The a -Si structure generated by the Tersoff potential contained defects consisting of the five coordination and the concentration decreased with the cooling rate. More extensive study is needed to clarify the dominant structural defect and ESR active site in a -Si.

ACKNOWLEDGMENTS

This work was conducted as JSPS Research for the Future Program in the Area of Atomic-Scale Surface and Interface Dynamics. We would like to thank T. Kumamoto and K. Yoshida for their assistance on molecular-dynamics calculations. Part of this work is the result of "Technology for Production of High Quality Crystal," which is supported by the New Energy and Industrial Technology Development Organization through the Japan Space Utilization Promotion Center in the program of the Ministry of International Trade and Industry.

- ¹For example, see T. Motooka, *Thin Solid Films* **272**, 235 (1996).
- ²R. Car and M. Parrinello, *Phys. Rev. Lett.* **60**, 204 (1988).
- ³I. Stich, R. Car, and M. Parrinello, *Phys. Rev. B* **44**, 11 092 (1991).
- ⁴J. Fortner and J. S. Lannin, *Phys. Rev. B* **39**, 5527 (1989).
- ⁵S. Kugler, G. Molnár, G. Petö, E. Zsoldos, L. Rosta, A. Menelle, and R. Bellissent, *Phys. Rev. B* **40**, 8030 (1989).
- ⁶W. A. Kamitakahara, H. R. Shank, J. F. McClelland, U. Buchenau, F. Gompf, and L. Pintschovins, *Phys. Rev. Lett.* **52**, 644 (1984).
- ⁷For example, see H. Balamane, T. Halicioglu, and W. A. Tiller, *Phys. Rev. B* **46**, 2250 (1992), and references therein.
- ⁸W. D. Luedtke and U. Landman, *Phys. Rev. B* **37**, 4656 (1988).
- ⁹W. D. Luedtke and U. Landman, *Phys. Rev. B* **40**, 1164 (1989).
- ¹⁰F. H. Stillinger and T. A. Weber, *Phys. Rev. B* **31**, 5262 (1985).
- ¹¹I. Stich, R. Car, and M. Parrinello, *Phys. Rev. B* **44**, 4262 (1991).
- ¹²J. Tersoff, *Phys. Rev. B* **38**, 9902 (1988).
- ¹³J. Tersoff, *Phys. Rev. B* **39**, 5566 (1989).
- ¹⁴M. Ishimaru, K. Yoshida, and T. Motooka, *Phys. Rev. B* **53**, 7176 (1996).
- ¹⁵M. Ishimaru, K. Yoshida, T. Kumamoto, and T. Motooka, *Phys. Rev. B* **54**, 4638 (1996).
- ¹⁶S. J. Cook and P. Clancy, *Phys. Rev. B* **47**, 7686 (1993).
- ¹⁷K. Binder and D. W. Heerman, *Monte Carlo Simulation in Statistical Physics, An Introduction* (Springer, Berlin, 1988).
- ¹⁸R. Zallen, *The Physics of Amorphous Solids* (Wiley, New York, 1983).
- ¹⁹P. Baeri, G. Foti, J. M. Poate, and A. G. Cullis, *Phys. Rev. Lett.* **45**, 2036 (1980).
- ²⁰P. C. Kelires and J. Tersoff, *Phys. Rev. Lett.* **61**, 562 (1988).
- ²¹M. D. Kluge, J. R. Ray, and A. Rahman, *Phys. Rev. B* **36**, 4234 (1987).
- ²²S. T. Pantelides, *Phys. Rev. Lett.* **57**, 2979 (1986).
- ²³I. Stich, M. Parrinello, and J. M. Holender, *Phys. Rev. Lett.* **76**, 2077 (1996).
- ²⁴W. A. Kamitakahara, C. M. Soukoulis, H. R. Shanks, U. Buchenau, and G. S. Grest, *Phys. Rev. B* **36**, 6539 (1987).